Magnet-Targeted Delivery and Imaging

P. Stephen Patrick, Quentin A. Pankhurst, Christopher Payne, Tammy L. Kalber*, and Mark F. Lythgoe*

1   Introduction

Magnetic nanoparticles, in combination with applied magnetic fields, can non-invasively focus delivery of small-molecule drugs and human cells to specific regions of the anatomy. This emerging technology could solve one of the main challenges in therapy development: delivery of a high concentration of the therapeutic agent to the target organ or tissue whilst reducing systemic dosing and off-target side effects. Several challenges, however, must be met before this technology can be applied either effectively or safely in the clinic to augment therapies.

Multiple nanoparticle features interact to influence the efficiency of magnet-targeted delivery, and so their design will have a large influence on the success of therapeutic targeting. For example iron oxide core size and composition affect the type (superparamagnetism/ferrimagnetism/antiferromagnetism) and strength of magnetism, and thus the amount of force that can be applied by an external magnetic field. Furthermore, particle behaviour within biological systems can be affected by particle size and coating, including their cell uptake, extravasation rate, circulation time, clearance, aggregation, and degradation.

To assess the impact of these factors on particle biodistribution and success of delivery, it is useful to be able to image nanoparticles non-invasively with a clinically

---

*Author contributed equally with all other contributors.

P.S. Patrick • C. Payne • T.L. Kalber • M.F. Lythgoe (✉)
Division of Medicine, UCL Centre of Advanced Biomedical Imaging, University College London, Paul O'Gorman Building, 72 Huntley Street, London WC1E 6DD, UK
e-mail: m.lythgoe@ucl.ac.uk

Q.A. Pankhurst
UCL Healthcare Biomagnetics Laboratory, University College London,
21 Albemarle Street, London W1S 4BS, UK

available imaging modality. One solution to this is the use of magnetic resonance imaging (MRI), which is sensitive to the presence of magnetic particles, such as iron oxide, in most biological tissue. This can give high-resolution anatomical information on particle location, providing a translatable method to confirm delivery success. However, MRI lacks the quantitative ability to assess whole-body biodistribution, and so the incorporation of other imaging agents, such as radionuclides, into particles could also be beneficial (see Chap. 10).

Preclinical researchers have investigated the use of magnetic targeting-based therapies across a wide range of conditions, and positive results have been reported [1, 2]. Furthermore, improved drug delivery to tumours has been demonstrated in the small number of clinical trials completed to date [3, 4]. Other potential cancer therapy applications include embolization and the delivery of radiotherapy agents, as well as the heating of targeted magnetic particles using alternating current magnetic fields for hyperthermia-based treatment or the controlled release of drugs [5]. For regenerative medicine, stem and progenitor cells have been targeted to specific organs such as the heart and brain to restore function to damaged tissue in mice and rats [6]. In the emerging field of "micro-robotics," bacteria, magnetic particles, and microsurgical robots have been directed through the vasculature or organs in live animals or mazes using computer-interfaced magnetic devices and real-time MRI to follow their progress [7–10].

In this chapter, we provide a basic introduction to the physical principles behind magnetic targeting technology, relevant design features of nanoparticles and magnetic targeting devices, an overview of preclinical and clinical applications, and an introduction to imaging magnetic particles in vivo.

2 General Physical Principles

The magnitude and direction of force that can be exerted on a magnetic particle will determine its potential to be targeted. In general terms, this force depends only on the magnetisation of the particle (M), and the strength and spatial distribution of the magnetic field (B), as described by (1)

$$F_m = \left(M \times \nabla \right) B \tag{1}$$

In this, and the following equations, it is important to note that we are dealing with three-dimensional vectors that describe the resulting magnetic force, as well as the magnetic field and gradient; so for example $\nabla = \left(\dfrac{\partial}{\partial x}, \dfrac{\partial}{\partial y}, \dfrac{\partial}{\partial z} \right)$ is the vector gradient operator, and $\left(M \times \nabla \right)$ is a $\left(3 \times 3 \right)$ matrix with elements $M_x \dfrac{\partial}{\partial x}$, etc. In small magnetic fields, where M is linearly proportional to the applied magnetic field, Eq. (1) may be written as [1]

$$F_m = \frac{\Delta \chi \, V_m}{\mu_o} \left(B \times \nabla \right) B \tag{2}$$

where μ_o is the magnetic permeability constant of free space. The other variables are explained in more detail below:

$$\Delta\chi$$

The relative magnetic susceptibility of the particle: This can be understood as a ratio of the induced magnetisation to the strength of the inducing field, and is characteristic for each type of magnetic particle in a given arrangement. During targeting experiments, the amount of force that can be exerted on the particle is proportional to $\Delta\chi$, which is the difference between the magnetic susceptibility of the particle and that of the external medium. As the susceptibility of normal biological tissue and fluids, such as the blood, is usually negligible in comparison to the particle, $\Delta\chi$ is typically equivalent to the magnetic susceptibility χ of the particle.

$$V_m$$

The volume of the magnetic particle: (Note that we use "particle" to denote the magnetic entity that is being actuated, and that this may be a multicomponent entity, e.g. one in which many inorganic magnetic cores may be encapsulated in an organic matrix.) In cases where a cell or magnetoliposome is loaded with multiple magnetic particles and an aggregation of magnetic particles exists, the particles will typically behave as a single magnetic particle. For simplification the volume of the particles in this situation can be summed to estimate the force acting upon them:

$$\left(B\times\nabla\right)B$$

The external magnetic field—both its strength, $B = |B|$, and its spatial variation (commonly referred to as the "magnetic field gradient"), as expressed by the vector product with the gradient operator: The amount of force that can be applied to a magnetic particle is proportional to the field strength, up to field strengths that approach the saturation magnetisation (Fig. 1a) for a given particle (typically $0.5 < B < 1.0$ T). Field strength depends on the strength of the magnetic device and the position of the particle relative to the magnetic field created by the device. The magnetic field gradient depends on the shape of the magnetic field that is produced by the magnetic targeting device, and the position of the particle within the field. The direction of the gradient is the main controllable parameter that will determine the direction of particle movement. In a uniform magnetic field lacking a gradient, the directional magnetic force acting upon a particle will be negligible.

As the magnetic force acting on a particle is only linearly dependent on magnetic field strength over a certain range, Eq. (2) is not applicable for higher magnetic field environments, where the particle approaches its saturation magnetisation, M_s. This can be visualised on the hysteresis curve (Fig. 1), which shows the induced magnetism of a magnetic particle on the y-axis in response to increasing external magnetic field strength along the x-axis. At higher field strengths, another approximation can be used to estimate the force [11]:
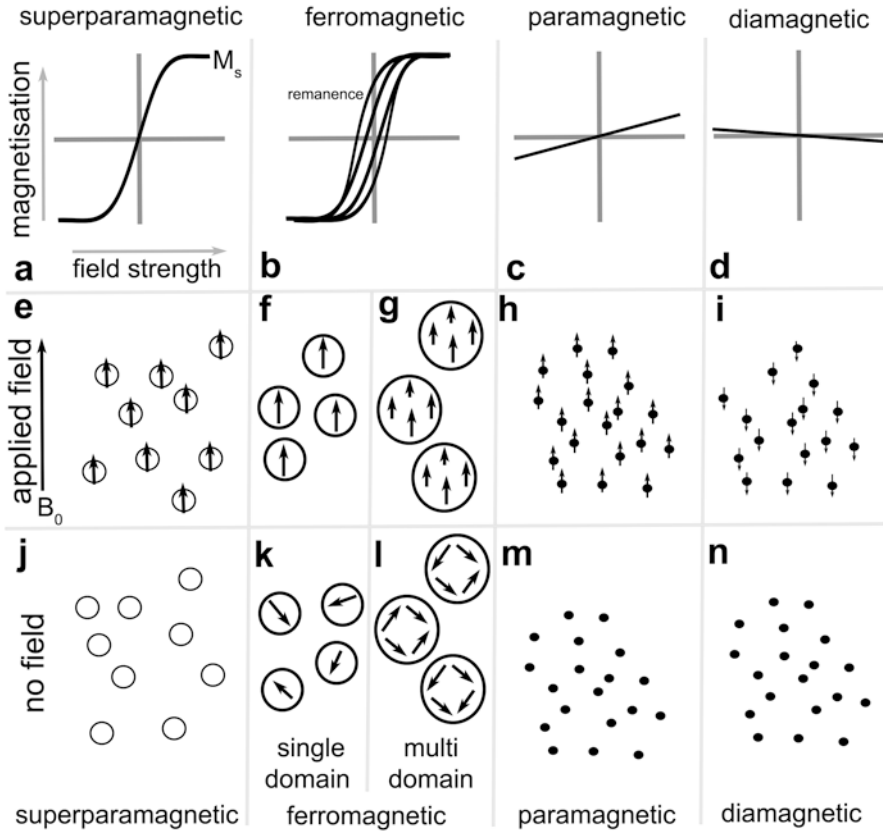
Fig. 1 Hysteresis curves showing net particle magnetisation induced by varying external field strength, for (**a**) superparamagnetic, (**b**) ferromagnetic (or ferrimagnetic), (**c**) paramagnetic, and (**d**) diamagnetic materials. Particle magnetisation in an applied field for (**e**) superparamagnetic, (**f**) single-domain ferromagnetic (or ferrimagnetic), (**g**) multi-domain ferromagnetic (or ferrimagnetic), (**h**) paramagnetic, and (**i**) diamagnetic materials. Net magnetisation in the absence of a magnetic field for (**j**) superparamagnetic, (**k**) single-domain ferromagnetic, (**l**) multi-domain ferromagnetic, (**m**) paramagnetic, and (**n**) diamagnetic materials. Further explanations on the different forms of magnetism can be found in Sect. 3.1

$$F_m = \frac{V_m M_s L(x)}{\mu_o B}(B \times \nabla)B \tag{3}$$

where $L(x) = \coth(x) - \frac{1}{x}$ is the Langevin function for $x = \mu_o V_m M_s B / k_B T$, k_B is Boltzmann's constant, and T is temperature. By incorporating the Langevin function into this equation, it becomes possible to model the sigmoidal induction of magnetisation in response to increasing field strength seen on the hysteresis curve (Fig. 1), overcoming the assumption of linearity in Eq. (2). This allows Eq. (3) to be used for any field strength. Please see Riegler et al. for further details [11].

Table 1 Bulk saturation magnetisation for selected minerals and metals/alloys at room temperature [12]

Composition	Magnetic order	M_s (emu/g)
Fe_3O_4	Ferrimagnetic	90–92
γ-Fe_2O_3	Ferrimagnetic	70–80
α-Fe_2O_3	Canted-antiferromagnetic	0.4
$CoFe_2O_4$	Ferrimagnetic	80
$MnFe_2O_4$	Ferrimagnetic	77
$NiFe_2O_4$	Ferrimagnetic	51
Co	Ferromagnetic	161
CoFe	Ferromagnetic	235
Fe	Ferromagnetic	218
Ni	Ferromagnetic	55
Ni_3Fe	Ferromagnetic	120

(Note that size and surface effects may lead to lower M_s values in nanoparticulate materials than those listed here.) Most magnetic particles used for biomedical applications are iron oxide based, and consist of either maghemite or magnetite. Nanoparticles made from metal alloys such as CoFe would have greater saturation magnetisation than iron oxides, potentially providing more force at high field strengths

As the saturation magnetisation becomes relevant at higher field strength, this might influence the choice of magnetic material used. Of the two most common types of iron oxide used in magnetic particles, magnetite (Fe_3O_4) typically has higher saturation magnetism than maghemite (γ-Fe_2O_3), though higher values are found in some metals and alloys (Table 1).

Counteracting the magnetic force, targeting efficiency will be affected by additional physical parameters specific to the precise anatomical context, including fluid velocity (v_w) and viscosity (η), difference in particle or cell velocity and fluid velocity (Δv), and particle or cell radius (R_m). These can be used to calculate the drag force acting on the particle and against the magnetic force that is exerted on a particle within a given fluid [1]:

$$F_d = 6\pi\eta R_m \Delta v$$

As drag force is proportional to the surface area of a particle, smaller particles will experience greater drag per unit volume than larger particles or particle-loaded cells or liposomes. Therefore the resulting force will be proportionally greater the larger the object to be targeted, assuming that it is well loaded with magnetic particles. Though in general this means that larger magnetic particles and particle-loaded entities will be targeted more effectively in the vasculature, in some circumstances this might be offset to a degree by certain advantages of smaller particles, such as increased extravasation and diffusion rate through certain tissues, which is discussed in part 3.4 of this chapter. Mathematical modelling of the forces affecting magnetic particle targeting in biological tissues has been further explored by Nacev et al. [12].

3 Magnetic Particles

3.1 *Particle Size and Magnetism*

Core size and material affect the type and potential strength of magnetism that a particle displays (Fig. 2), which in turn influences how it behaves in magnetic targeting applications. (Temperature also has a significant effect, but in this chapter it should be taken as read that the ambient temperature is in the room/body temperature range.) In the low nanometre range (up to 2–30 nm depending on the material [13]) most iron-, nickel-, and cobalt-based magnetic materials are superparamagnetic—they are magnetic only in the presence of an external magnetic field, and their magnetism increases with external magnetic field strength up to their saturation magnetisation (Fig. 1 a, e, j).

Up to a higher size limit (50–100 nm, again dependent on the material [13]) the same materials will possess a single magnetic domain (Fig. 1 b, f, k). When a particle is in the single-domain state, its internal magnetisation is aligned in the same direction, whereas in multi-domain particles each domain may point in a different direction. In the application of a magnetic field, individual single-domain magnetic particles do not increase their magnetisation, which remains at saturation (M_s); however, multiple neighbouring particles that are initially magnetised in varying directions (along their easy axis of magnetisation) will align with the magnetic field in chains (if in solution), or against their easy axis if they are not free to rotate. This increases the net magnetisation of the group and therefore the amount of directional magnetic force that can be applied to the particles by a field gradient.

At larger sizes, the magnetic cores will split into multiple non-aligned domains to reduce the internal energy of the particle (Fig. 1g, l). These are known as multi-domain magnetic particles. Domain wall motion can be induced by an external field

Fig. 2 Particle core size and material determine whether particles display superparamagnetism, single-domain or multi-domain ferromagnetism/ferrimagnetism [13]
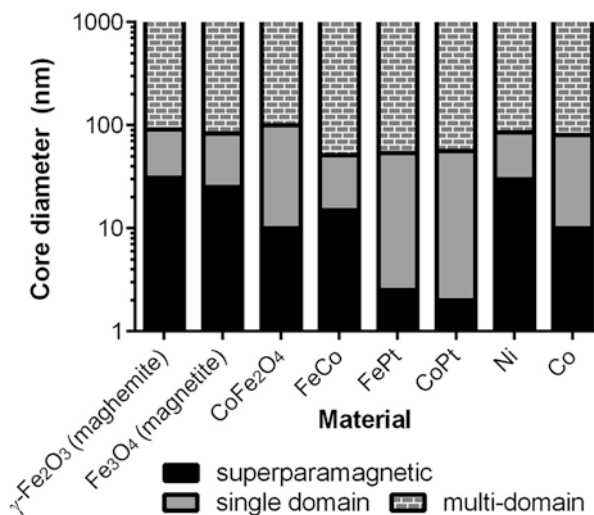
to increase the net magnetisation, with domains that are magnetised in directions favoured by the applied field growing at the expense of unfavourably oriented domains, and saturation magnetisation may be reached if a sufficiently strong external field is applied. The field strength at which this is achieved, and the retention of magnetic domain alignment after removal of an external magnetic field (known as remanence), can be determined from a hysteresis curve for the particles (Fig. 1). Though the same net effect is seen in groups of single-domain particles due to magnetic anisotropy, this is due to different underlying reasons as illustrated in Fig. 1.

The magnetic susceptibility of a given assembly of particles is influenced by the above factors, such as the composition and magnetic structure of the particle core. Magnetic susceptibility is important for targeting applications, as it is proportional to the amount of magnetic force that can be applied below field strengths at which the magnetisation is saturated. This can also be visualised on a hysteresis curve (Fig. 1). This allows us to compare magnetic properties for several potential candidate magnetic particles to determine which will be most suitable for a specific magnetic targeting application. This is particularly important when considering nanoparticles originally made for use as MRI contrast agents (superparamagnetic iron oxide particles—SPIOs), which were not designed for the effective production of force, but for their ability to produce local magnetic field inhomogeneities resulting in areas of hypo-intensity in T_2-weighted MR images (due to de-phasing of the surrounding ^{1}H proton spins). For this reason, some MRI contrast agents are not well suited for certain magnetic targeting applications due to their small core size, especially the ultra-small SPIOs or USPIOs.

Despite this potential mismatch in required design features between the two applications, some SPIOs designed as MRI contrast agents do have suitable properties for particular magnetic targeting applications. Among these are some of the SPIO particles approved for human use by the FDA, Endorem (Feridex), and Ferucarbotran (Resovist), which have both been used successfully for a number of preclinical magnetic targeting studies [2] (Table 2). Furthermore, most commercially available SPIOs have been designed for low toxicity and good cell uptake and stability, which also suits them to both cell tracking with MRI and magnetic targeting applications that use cells.

3.2 Particle Aggregation

Particle aggregation can be promoted by both biological and magnetic factors, and might be beneficial or detrimental according to the type of magnetic targeting application and the duration and scale of aggregation. As superparamagnetic particles are magnetic only in the presence of a magnetic field, they will not magnetically aggregate in zero field. However, temporary chains of superparamagnetic particles can form at sufficiently high concentration and field strength as a result of attractive dipole-dipole interactions [14]. Permanent magnetic particles however will cluster together in the absence of an external magnetic field, and will form chains parallel

Table 2 Selection of particles used for magnetic targeting of cells

Particle name	Hydrodynamic diameter	Organs targeted	Cell types used	Core type	Reference(s)
Feridex/Endorem	80–150 nm	Brain, knee joint cartilage, liver, spinal cord, vasculature	hNSC, MSC, BMSC, EPC, MNC	Multiple (5–6 nm) superparamagnetic cores	[15–20]
Resovist/Ferucarbotran	62 nm	Femur, heart, skeletal muscle	MSC	Multiple 3–5 nm superparamagnetic cores	[21–23]
Feraheme/ferumoxytol	17–31 nm	Heart	CDC	6–8 nm Superparamagnetic core	[24]
FluidMag	50, 100, and 200 nm	Retina, vasculature	MSC	Multiple superparamagnetic cores	[25, 26]
Biomag/superparamagnetic microspheres	0.5–2 μm	Arteries, heart, vasculature	EC, CDC, MNC,	Multi-domain permanent magnetic core (0.5–2 μm)	[20, 27]
Magnetospirillum sp.-derived particles	~40 nm	Hind limb	EPC	Single-domain permanent magnetic core (~40 nm)	[28]
Multifunctional upconversion nanoparticles	240 nm	Skin wound	MSC	Multiple 5 nm superparamagnetic cores	[29]

Clinically approved particles listed in bold type, commercially available particles shown in italics. *hNSC* human neural stem cell, *MSC* mesenchymal stem cell, *BMSC* bone marrow stromal cells, *EPC* endothelial progenitor cell, *MNC* mononuclear cell, *EC* endothelial cells, *CDC* cardiosphere-derived cells

to an applied external field. Clustering and the formation of chains in particles and particle-loaded cells are also dependent on their concentration, surface charge and chemistry, and viscosity and flow rate of the solution. This can be modelled for a given scenario to predict the optimal parameters to use [30, 31].

For some applications requiring the production of vascular embolisms, particle aggregation is desirable, and larger magnetic particles into the micron range or above have been used for this purpose [32, 33]. For other applications such as drug or cell delivery that require even distribution throughout a tissue and efficient extravasation, aggregation will impede delivery and so the use of smaller single-domain or superparamagnetic particles might be more effective [34]. However, the tendency of particles to form temporary chains or small aggregations during delivery will increase the amount of force that can be applied by an external field and can increase targeting efficiency, so this must be balanced against the probability of embolization to achieve optimum delivery. In addition to tuning particle size, the balance between the application of sufficient force and the possibility of embolization can be achieved by assessing a range of targeting device field strengths for a given application [22].

Recent work has also suggested that microfabricated particles comprising multi-layer stacks of alternating magnetic and non-magnetic materials can be used to avoid aggregation. These can be produced with diameters on the scale of multido-main ferromagnetic particles (2 μm), but with zero remanence, and with an efficient switch to saturation magnetisation upon application of a given field strength [35]. This avoids some of the limitations associated with the aggregation of larger parti-cles while retaining many of the benefits including the higher amount of force that can be applied per particle and increased circulation times (Sect. 3.4). The construc-tion of larger composite particles from multiple small superparamagnetic cores can also avoid the magnetic aggregation typical of larger permanently magnetic parti-cles while retaining the benefit of higher magnetic force per surface area and thus increased overall targeting efficiency. Several other methods can achieve similar effects, including the creation of "nanoworms" from strings of particles [36, 37], or embedding multiple superparamagnetic cores within dextran [38] or silica coating [39], hydrogel, [40], vesicles [41], or magnetoliposomes [42].

3.3   Cell Uptake and Labelling

Particle size also affects cell uptake, and therefore the resulting amount of force that can be applied to a particle-loaded cell will be determined not only by the particle core size, but also by how many particles the cell has taken up. Around ten different biological mechanisms of particle uptake have been discovered in cells, and are active to varying degrees depending on the specific cell type and its environment, and the size, charge, and coating of the particle [43, 44]. These include non-specific uptake mechanisms such as macropinocytosis (particles around 1 μm) and caveolar-mediated endocytosis (for particles ~60 nm), as well as receptor-dependent mecha-nisms such as clathrin-mediated endocytosis (~120 nm) and clathrin-and

caveolin-independent endocytosis (~90 nm) [45]. Due to the complexity of cell uptake mechanisms, it is difficult therefore to predict with accuracy the range of particle sizes that will be taken up effectively by a given cell type, except for cells that have already been investigated with similar particles. Generally, particles between 20 and 200 nm in diameter are more effectively taken up by most non-phagocytic cell types than particles either side of that range [46–48], though increased particle charge will improve the uptake of larger particles into the micron scale [48]. In addition to this, other interacting variables such as particle shape, stiffness, and surface chemistry will affect the uptake. A complete discussion of this topic falls outside the scope of this chapter and the reader is referred to a recent comprehensive review [44].

As most commercially available and FDA-approved magnetic particles designed for imaging applications fall within this range of 20–200 nm, and have been optimised for cell uptake by size and surface coating, these have found successful use in several magnetic cell-targeting studies [2] and can be used for reference in designing particles for this purpose (Table 2).

When labelling adherent cells with magnetic particles, uptake can sometimes be promoted by application of a magnetic field. This has been demonstrated with a range of particle and cell types [49, 50]. Additionally, this technique can be used to simultaneously introduce DNA to the cell (known as magnetofection), which might be useful if the cells are to be used for gene therapy [51].

Addition of antibodies to the particle surface can also promote uptake or attachment to specific cell types, according to the choice of antibody. In this way, cells can be labelled either prior to implantation or in vivo. For example, antibody-labelled magnetic particles administered intravenously can label specific cell types within the circulation, allowing these cells to be magnetically targeted to specific locations within the body for therapeutic purposes. This strategy has been demonstrated to improve repair of infarct myocardium using circulating stem cells [6]. Here a dual mechanism of targeting was demonstrated, in which cells were targeted to the heart using a magnetic field, and also by the particles that displayed antibodies for both the stem cell and for the damaged cardiac tissue. As this approach required only the intravenous administration of the particles, translation would be more straightforward than in therapies in which cells must be harvested, isolated, and labelled before being given to the patient. This strategy might also prove effective for magnetic targeting of antibody-based drugs, or together with the delivery of other small-molecule drugs or therapeutics such as siRNA (see Chap. 7) contained in magneto-liposomes or adsorbed to the particle surface.

3.4   Targeting Particles for Drug and Therapeutic Delivery

The required design features of particles that are to be used directly for therapy differ from those that are to be used to label cells, as do the constraints on these. This is due to several biological and physical factors.

For example, particle size affects extravasation rate and diffusion though tissue, and will affect the ability to target regions distant to the vasculature. This may be a particular concern for certain applications such as drug delivery to poorly vascularised metastases, or the targeting of particles for hyperthermia therapy. The effect of particle size on diffusion and extravasation can be modelled in a number of ways, and used to predict the range of particle sizes that might benefit from magnetic targeting, or which would be effective in a given tissue. In cases where particle size falls outside this range (20–400 nm, based on a simulation of tumour tissue), delivery by endogenous diffusion mechanisms might prove superior to targeting strategies [34].

Clearance of particles by the reticuloendothelial system (RES) and renal filtration are also dependent on size. Renal filtration will quickly clear the majority of circulating particles under 5 nm, but barely any that are above 9 nm [52]. Larger particles can be cleared by immune cells including Kupffer cells in the liver, monocytes, spleen, and macrophages, which engulf nanometre- to micron-sized particles, decreasing delivery to the target organ. Targeting efficiency will therefore be improved the faster the particles can be attracted to the target site, before clearance has occurred, though this may be challenging when most particles are cleared on the first-pass circulation post-injection. The rate at which particles are scavenged in this way is affected by their coating and size. It is outside the scope of this chapter to review this topic in detail, but several modifications can reduce RES uptake such as polyethylene glycan (PEG) coating, which has been demonstrated to enhance the circulation time of particles and improve magnetic targeting efficiency [53]. The utility of PEGylation in reducing RES uptake is further illustrated by the results achieved with Doxil—a liposomal formulation of doxorubicin, and the first nano-encapsulated drug to obtain clinical approval [54].

Another strategy in reducing RES uptake utilises the properties of red blood cells, which naturally evade clearance and achieve long circulation times through a combination of their size, surface composition, and charge. For this reason they have been used in magnetic targeting applications for drug delivery [55, 56]. In one study red blood cells were loaded with a drug for photodynamic therapy and targeted to the tumour, resulting in a decrease in tumour volume following phototherapy compared to non-magnetically targeted control conditions [56]. In an adaptation of this concept, nanoparticles can be coated with extracted cell membrane of red blood cells, thereby "cloaking" the underlying material. This provides a strategy to utilise the unique binding properties of red blood cells to diseased tissue and pathogens [57], and could facilitate particle-based drug delivery to sites of inflammation in combination with magnetic targeting.

On the other hand, several iron oxide contrast agents for MRI, including those that have been clinically approved, were originally designed with size and surface coatings to optimise their uptake by the RES, for the purpose of imaging uptake in the liver. These might not therefore be optimal for magnet-targeted delivery of drugs due to their increased clearance rate.

To bypass normal clearance mechanisms, several magnetic targeting studies have opted for local delivery to the target organ using a directed injection [4, 26, 58], instead of a systemic injection. For example in a clinical trial targeting hepato-

cellular carcinoma, particles were injected via a catheter inserted into the hepatic artery, which could be moved intraoperatively between the acquisition of magnetic resonance images to ensure that particles were effectively delivered to the entire tumour (Fig. 3) [3]. This strategy can reduce the number of particles or cells that can be cleared by the RES prior to reaching the site of interest, increasing the efficiency of delivery. Though this approach increases the invasiveness of the technique, it may be required in several situations to achieve effective delivery. However, some difficult-to-target organs such as the brain have been efficiently targeted using a systemic intravenous injection of particles [38], though this may depend on blood-brain-barrier breakdown related to specific disease states. Together, these results suggest that both systemic and local delivery can be effective.
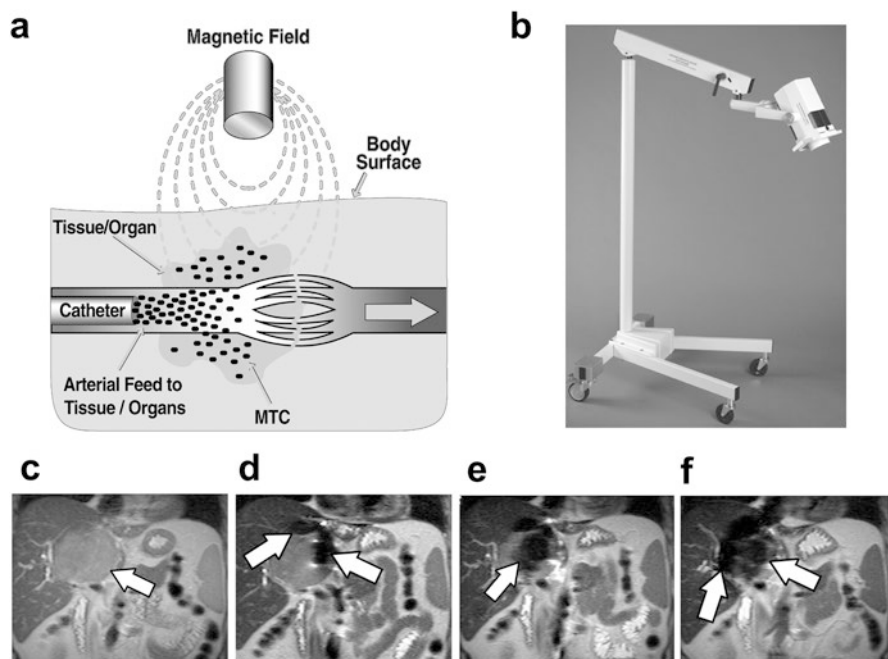

Fig. 3 (**a**) Diagram depicts the mode of action of magnetic targeted therapy. After leaving the intra-arterial catheter, magnetically targeted carrier (MTC) doxorubicin is drawn out of the artery into surrounding tumour and/or liver tissue by the influence of the local magnetic field (image courtesy of FeRx). (**b**) 5 kG portable magnet used for magnetic targeted therapy. The overall height of the magnet and holding apparatus is 1.4 m. (**c**–**f**) Coronal single-shot spin-echo MR images (839/80, one signal acquired, 6 mm section thickness) obtained, **c**, before MTC-DOX administration and, **d**, after the first, **e**, the second, and, **f**, the third dose of MTC-DOX. The selective hepatic arterial catheter was repositioned between each dose [3]. Figure reproduced from Wilson et al. Hepatocellular carcinoma: Regional therapy with a magnetic targeted carrier bound to Doxorubicin in a dual MR imaging/conventional angiography suite—Initial experience with four patients. Radiology 2004;230:287–293, with permission from the Radiological Society of North America

Particle size also affects the surface area-to-volume ratio, which is relevant to the adsorption of drugs to the particle surface. However, there is a trade-off between the motivations of using smaller particles, and the increased force that can be gained from using larger particles, and so a range of particle sizes can be considered. For example, magnet-targeted drug delivery in the clinic has been trialled across a scale of particle sizes: 100 nm particles coated with glucose and bound to epirubicin [4], and 0.5–5 µm sized particles with an activated carbon coating bound to doxorubicin [3]. Even larger metallic objects in the millimetre scale have been used for targeting and hyperthermia therapy, which does not require the same extent of extravasation and distribution of particles, due to transfer of heat across tissue [7].

For targeting tumours, particle retention can be improved by the enhanced permeability and retention (EPR) effect, which has been well documented to improve delivery [59]. As this effect relies on leaky vasculature and diffusion of particles through the extracellular space, it is a size-specific phenomenon, with the enhancement of particle retention decreasing with particle diameters above 30 nm in one tumour model [60], though this will differ to some degree depending on tumour type and nature of its vascularisation. Though enhanced nanoparticle delivery is achievable in difficult-to-access sites, such as brain tumours with magnetic targeting [61], one limitation of magnetic targeting for cancer treatment is the issue of metastases, which can be remote, disperse, and difficult to identify. These factors would limit the ability for targeting to be used, as they might require a separate targeting field to be applied for each site that could be identified.

For drug delivery it is also necessary to consider the attachment of cargo to the particle. In the simplest form this can rely on absorption of the drug onto the particle surface [3, 4]. However controlled release of the drug can be achieved if it is trapped in a solid coating, such as silica, around the magnetic particle. By heating the particle using a focused alternating field around the target tissue, as during a hyperthermia treatment, the coating can be made to melt, thereby releasing the drug [5, 41]. Similar strategies can be employed to release drugs from magnetoliposomes [62].

4   Magnetic Devices for In Vivo Targeting

Appropriate selection or design of magnetic targeting devices depends largely on the anatomical region to be targeted. Other considerations include the sort of particle that will be targeted (small superparamagnetic particles will typically require a stronger magnetic field and field gradient to exert the same force on them than larger or permanent single-magnetic-domain particles), as well as the type of steering and/or imaging that is required for the application. Several broad categories of magnetic targeting device will now be discussed, including their benefits, limitations, and applications to which they are suited.

4.1 Permanent Magnets

Small permanent magnets have found wide use in preclinical magnetic targeting studies, as they are readily available and provide high field strengths and gradients over a relatively small area, without the larger hardware size or cooling required for electromagnets. While suitable for tissue depths of a few centimetres, the limited spatial extent of such fields would restrict their external use in the clinic to targeting superficial tissue [3, 4], unless the particles are delivered to the internal site by direct injection (Fig. 3). Furthermore, a single permanent magnet cannot produce a local maximum of field gradient within the patient (unless surgically implanted—see below), meaning that for practical purposes that magnetic particles will be attracted from the inside of the patient to the surface of the magnet to produce a focal accumulation towards the skin, rather than vice versa. This makes it difficult to target an internal location non-invasively or achieve an even distribution of particles throughout a target organ. One solution to this is to change the location of the magnet during the targeting procedure, for example from one side of the liver to the other, so that the targeted particles are more evenly spread out [34]. This was demonstrated ex vivo to increase the concentration of magnetic particles within poorly perfused liver metastases by 1.8-fold above diffusion alone, and was predicted to be effective for particles in the 30–500 nm diameter range, with normal diffusion acting more effectively than targeting for smaller particles [34]. Another option is the implantation [18] or stereotactic insertion of magnets [32, 33]. While this can achieve effective targeting to internal organs, it does not completely avoid the invasive procedures associated with more traditional surgical implantation methods. Alternatively, magnetic stents can be manoeuvred to a specific point of the vasculature to achieve targeting of cells or particles [63], but again this is invasive and only useful for targeting areas that are accessible in this way.

4.2 Permanent Magnet Arrays

By superimposing two or more magnetic fields in an array of permanent magnets, some of the limitations of single permanent magnets can be overcome to produce more complex field shapes and gradients. With certain configurations this can allow the device to remain external to the target tissue and steer magnetic particles away from the magnet itself. A simple example is two bar magnets that have been arranged so that their fields overlap to create a remote point from which magnetic particles are pushed away from the magnet (Fig. 4). This has been posited as a solution for magnetically "injecting" nanomedicines into the inner ear [64], and has been validated in a rat model over distances relevant to use in the human ear [65]. This is important as the ear is behind the blood-brain barrier and can be a difficult organ in which to achieve drug delivery. It is also protected by the tympanic, round window, and oval membranes, and magnetic targeting using a "pulling" magnetic field from the opposite side of the head would require an unfeasibly strong magnetic field to achieve the same amount of force [64].

Fig. 4 (**a**) Two permanent magnets arranged at an angle can create a remote focal point about which magnetic particles may be repelled. (**b**) This magnet configuration has been proposed as a way to deliver magnetic particles to deep-tissue locations such as the inner ear [63, 64]. (**c**) Cylindrical Halbach array of permanent magnets [26], where the *arrows* show the direction of force. (**d**) The Halbach array pictured in (**c**) can be used to retain therapeutic cells within the vasculature, providing potential regenerative effects in cases of peripheral limb ischemia [11, 26]
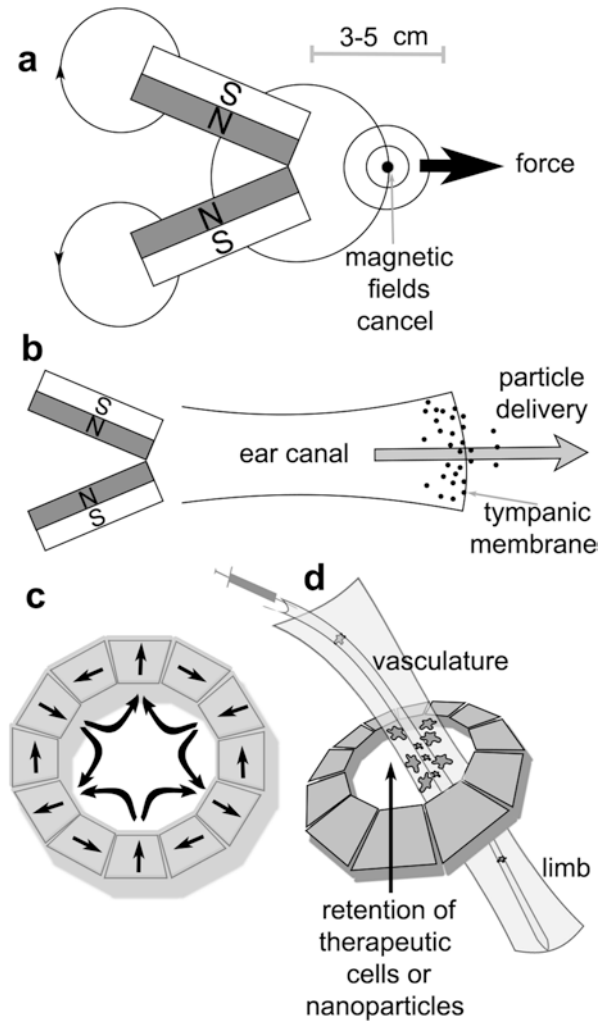
Using the same principles an optimal 2D Halbach array of 36 magnets was computationally designed to create a pushing force at 10 cm distance with nine times the force achievable with only two magnets of the same overall volume and field strength [66]. These results hold promise for the development of relevant clinical devices, as one of the challenges in translating preclinical results will be scaling up the technology for use with greater tissue depths.

As well as increasing the magnetic pushing force that can be applied at a specific point, 2D and 3D Halbach arrays can also be designed to increase the attractive force from permanent magnets [66]. A relevant example is the Halbach cylinder [26], which is a circular array of permanent magnets that can be built to fit around a limb and target cells or magnetic particles for retention within a specific portion of

the vasculature (Fig. 4c, d). This has been suggested as a good solution to achieve targeting of therapeutic cells for peripheral limb ischemia [11, 26]—currently one of the largest disease areas being investigated in clinical cell therapy trials.

Though arrays of permanent magnets are a promising solution to several applications due to their relatively low cost, size, and ease of operation, several limitations apply. One of the most important of these is predicted in Earnshaw's theorem, which holds that for most situations relevant here, no arrangement of static magnetic fields will create a remote focal area in the magnetic field in which magnetic particles will accumulate. The next section will discuss electromagnets, which can be used to work around this limitation.

4.3   Electromagnet-Based Arrays

Using computer-interfaced control, electromagnet-based systems can produce switchable and tuneable field gradients to direct magnetic particles along a three-dimensional route controlled in real time. This can be illustrated by several working examples, including a "magnetic stereotaxis" system based on four electromagnets which was capable of guiding a magnetic pellet along a defined route within a live dog brain to enable hyperthermia treatment of a glioma [7]. In a development of this system, a clinical sized magnetic stereotaxis device based on six superconducting coils was built, and validated on a gelatin brain phantom [67]. X-ray imaging capability in this device allowed particle movement to be monitored intraoperatively, so that feedback adjustments could be made to steer and improve navigational accuracy. This type of image-guided, focused non-invasive tumour ablation is currently only achievable with radiosurgical techniques such as "gamma-knife" therapy, which are prone to damage the healthy surrounding tissue, whereas a targeted hyperthermia-based treatment might avoid this due to the higher heat tolerance of normal tissue.

Computer-interfaced electromagnetic devices can also control much smaller magnetic devices on a fine scale, for example for steering micro-robots within the eye [9]. This has been demonstrated with control of both robot orientation and direction of movement, and is proposed as a solution to enable microsurgery and drug delivery in what is another difficult organ on which to operate. This was demonstrated during testing through the control of a magnet attached to a hypodermic needle, which was used to pierce a target blood vessel in vivo [9].

For control of multiple particles at once, as might be beneficial in a nanoparticle drug delivery system, an array of eight electromagnets was used together with a sequence of directional magnetic pulses to cause accumulation at an external focal site [68]. This technique made use of the ability of ferromagnetic rods to be rotated and moved by the application of external fields. More examples on particle delivery with electromagnets will be given in the next section, which will discuss the use of MRI scanners for targeting applications.

4.4   Targeting Using MRI Systems

Though designed for imaging and not particle manipulation, MRI scanners share several features with the purpose-built electromagnet-based targeting systems described in the previous section. Their high magnetic field strength and controllable field gradients have been used for a handful of targeting applications, while their imaging capability can provide feedback on particle location during delivery.

Proof-of-concept studies show in vitro that human cells loaded with magnetic particles can be targeted using unmodified preclinical MRI scanner gradients in vascular flow models [20]. Further work expanded upon this to steer oncolytic virus-producing, iron oxide-loaded macrophages to sites of pulmonary and prostate tumours in vivo, resulting in enhanced tumour necrosis [69]. Simultaneous targeting and imaging have also been achieved using an MRI scanner to control a millimetre-sized magnetic sphere within live pig vasculature [70], and to direct magnetotactic bacteria around a maze [8]. Magnetic drug-encapsulating particles have also been directed in this way to either the right or the left lobe of the rabbit liver, providing a potential treatment for tumour metastases, this time with the aid of additional gradients optimised for particle steering [58]. The use of MRI hardware for magnetic targeting is advantageous in that high-resolution imaging can be performed with the same equipment at intervals during the targeting experiment [8, 58, 70]. In this way, particle accumulation can be seen in near-real time, allowing feedback adjustments on the field gradient to improve targeting efficiency. One limitation to this approach is that the field gradients present in clinical MRI scanners typically have maximum values of 40–70 mT/m, which is an order of magnitude or two below those produced in some dedicated magnetic targeting devices [7, 67]. A solution to this is the addition of "propulsion" gradient sets to the MRI hardware without permanent modification to improve targeting ability [58], which can increase the amount of force that can be applied. In theory this would facilitate the translation of this technology to the clinic, as the majority of the necessary hardware is already in place.

5   Applications

To provide a general overview of what has been previously achieved and possible areas of future development or translation, in this section we will introduce some results reported in both clinical and preclinical magnetic targeting studies.

5.1   Magnet-Assisted Embolization for Aneurysm and Tumour Treatment

In the first clinical use of magnetic targeting (1966), metallic thrombi were produced to block ruptured aneurysms in the brain [32, 33]. Large carbonyl iron particles injected into the carotid artery or site of aneurysm were targeted to two magnets

placed around the aneurysm to create a focal magnetic field (62 mm diameter, 375–750 mm length), using a stereotactic frame and X-ray guidance. Thrombus formation upon particle aggregation within the aneurysm was confirmed by X-ray imaging. This involved less invasive surgery than established alternatives, as the magnetic probes were inserted through small-diameter burr holes in the skull instead of exposing the brain to the site of aneurysm. Importantly, remote aneurysms that were too far from the skull to be otherwise operable could also be targeted, and dozens of patients were successfully treated. In a later refinement to the technique, magnetic particles were mixed with a rapidly polymerising acrylic to stabilise the particle aggregation post-injection and prevent the original metallic thrombus fragmenting [71]. Following this work, the same group tested the idea of using magnetic emboli to occlude tumour vasculature, though this did not progress to clinical testing [72]. Interest in this technique has been recurrent, with recent work combining magnetic tumour embolization with the delivery of radiotherapy using yttrium-90-conjugated magnetic particles [73]. In another example, a clinical MRI scanner equipped with an additional "propulsion gradient" set was used to target the formation of magnetic particle emboli in either the right or the left lobes of rabbit liver [58]. This suggests that non-invasive targeting of emboli might be possible in the clinic with little modification to currently available hardware, and without the need for invasive probe insertion.

5.2 Cancer Hyperthermia

The low heat resistance of tumour cells compared to healthy normal tissue can facilitate their selective killing when the target cancerous area is heated [74]. This can be achieved using a number of methods including whole-body heating, heating of inserted probes, and heating of targeted magnetic nanoparticles using an alternating current magnetic field or radiofrequency (RF) field. The first clinical demonstration was described in 1957 in gastrointestinal tract lymph node metastases [75], in which magnetic particles were injected into the lymphatic system, and then heated using an RF field. Interest in hyperthermia continues, with a number of recent clinical studies investigating iron oxide nanoparticle hyperthermia with alternating current magnetic fields in prostate tumours [76] and glioblastoma [77]. These trials have relied on direct injection of the particles without magnetic targeting, and though preclinical work has suggested the combination of these two procedures, few convincing demonstrations have been performed to date [78]. One study of note, however, combined the three-dimensional magnetic steering of a small (mm scale) magnetic pellet through the brain of a dog, guided by magnetic resonance imaging to a specific location, followed by RF-induced heating of the pellet once it reached the target site [7]. This was suggested as a possible future treatment for malignant gliomas and for combination with radiotherapy delivery. Though this was achieved using a pellet several millimetres in size, histological analysis showed that the particle did not cause haemorrhaging along its path. Adaptation for use with smaller particles might be possible and remove the need for direct brain implantation of the particle. The suitability of different magnetic particle types for hyperthermia has been systematically evaluated here [79].

5.3 Cell Targeting for Regenerative Medicine

Stem, progenitor, and differentiated cells have the potential to treat a range of currently incurable and degenerative diseases by initiating regenerative or immune-modulatory effects within the host tissue. A handful of cell therapies have gained approval for clinical use during the last 10 years, and many thousands more are currently being assessed in clinical trials [80]. It has therefore been suggested that cell therapy could become the third main class of therapeutic alongside small-molecule drugs and biological macromolecules, such as antibodies [81]; however such progress will rely on developments within the field and in associated technologies.

For many conditions, cell therapies require efficient delivery of cells to the afflicted organ or tissue, and this may be challenging without invasive surgical techniques or repeated implantations. The combination of magnetic targeting with cell therapy offers a solution to this by improving cell delivery and retention, and has increased treatment response compared to non-targeted controls in several preclinical disease models including myocardial infarction, brain ischemia, damaged skeletal muscle, skin wounds, bone fracture, spinal cord damage, and restenosis [2] (Table 2).

It is unclear in many cases if stem cells contribute to repair by differentiating into the cell types needed to reconstitute healthy tissue, or if their effect is mediated by paracrine signalling factors or immune modulation. It is likely that at least in some cases a combination of these effects is required, and so the ability of cells to maintain a therapeutic phenotype after magnetic particle labelling should be considered, including their ability to migrate and differentiate. To this end, it has been shown that it is possible to load mesenchymal stem cells with enough iron oxide particles to achieve magnetic targeting while retaining their differentiation capacity for multiple lineages [26]. As the potential toxic effects of magnetic particles are dependent both on particle and cell type, as well as the concentration of the particles used to label the cells, this would need to be established for each specific case.

This, however, assumes that the isolated therapeutic cells are to be loaded with magnetic nanoparticles and then transplanted into the patient. Though this is the dominant paradigm for magnet-targeted cell therapy [2], another strategy has recently been demonstrated to avoid many of the associated challenges. Here, iron oxide particles were labelled with antibodies specific for circulating stem cells, and then injected intravenously. These bound to stem cells within the blood supply, which were then targeted to the heart with an external magnetic field [6]. As the magnetic particles also had antibodies for damaged heart tissue, the targeting was achieved with both molecular and spatial specificity, and did not require the time-consuming pre-isolation and labelling of stem cells *ex vivo*. Furthermore, a significant increase in regeneration of ischemic heart tissue was achieved, and tracking of the particles to the heart was demonstrated using MRI [6]. By changing the antibodies for cell type or tissue type, as well as altering the location of the external magnetic field, this strategy could be easily altered for repair of other tissues.

To replicate this success in the clinic, several challenges will need to be met, including the production of magnetic fields on the scale of the human anatomy, optimisation of field strength [22], and development of suitable magnetic particles

for labelling cells (Sect. 3.3). As a handful of magnetic particle types have already
been approved for clinical use as MRI contrast agents, the latter of these barriers to
translation is somewhat reduced (Table 2).

5.4   Drug Delivery

Drug delivery is currently one of the largest areas of magnetic targeting research
[82], and the only one within which more recent efforts have been made in the clinic
[3, 4]. It is also well suited for combination therapy, having the potential for use
with multiple drugs and therapy types such as hyperthermia [78], radiation therapy,
photodynamic therapy [56], and embolization [10]. The idea of magnetically target-
ing drugs emerged in the 1970s, with the suggestion of using magnetic particle-
loaded erythrocytes [55] or magnetic microspheres as carriers [83]. The first
preclinical demonstration of drug delivery showed that drug-carrying microspheres
could be targeted to a specific section of the rat tail [83]. In this case, a 100-fold
lower systemic dose of the targeted drug was needed as compared to the untargeted
drug, to achieve the same local concentration in the targeted tissue. Early applica-
tion of this technique to tumour treatment resulted in total remission in the targeted
group, while nearly all of the animals receiving a non-targeted treatment died [84].
By reducing dosing in off-target areas, this could in theory reduce many of the side
effects associated with chemotherapy while allowing higher doses to be achieved in
the tumour for increased therapeutic efficiency.

   The first of the two clinical assessments of drug delivery to tumours was a phase
I trial which gave 14 patients varying intravenous doses of 100 nm magnetic parti-
cles bound to epirubicin, with effective magnetic fields of 0.5–0.8 T applied to
tumours for 60–120 min. In four of these patients, delivery of magnetic particles
was visible as a discolouration of the tissue exposed to the magnetic field, and in all
but five of the patients the presence of the particles was detectable with T_2-weighted
MRI [4]. All patients tolerated the therapy well, with no indications of toxicity and
reduced side effects and plasma drug concentration compared to dosing with free
epirubicin. However, the study concluded that the treatment of further patients
would be needed to prove efficacy.

   In the more recent clinical study that used doxorubicin bound to 0.5–5 μm sized
particles injected into the tumour, four patients with hepatocellular carcinoma were
treated in a phase I/II trial. In this study, tumours were characterised using angiog-
raphy to identify the hepatic artery branch that supplied the tumour and for catheter
guidance. MRI was also used pre- and post-delivery of treatment to reveal the cov-
erage of the tumour with magnetic particles (Fig. 3). When particles were not deliv-
ered to the whole of the tumour, MRI was able to indicate this, allowing repositioning
of the catheter and a second or third dosage to achieve greater coverage (Fig. 3c–f).
This intraoperative assessment is a major advantage to using magnetic particle-
bound drugs, as this non-invasive assessment of drug delivery is not possible with
most traditional therapies.

Aside from cancer treatment, magnetic targeting has also been suggested as a method of delivery for anaesthetics such as lidocaine to the spine [85], and magnetic aerosols to the lung to treat a number of respiratory complaints [86], though progress in non-cancer applications has so far been limited.

5.5   Bacterial Targeting and Therapy

The concept of treating tumours with bacteria has been around for a number of decades, with effective oncolysis demonstrated in several human studies with non-pathogenic Clostridium species [87, 88]. Recent work indicates a renewed interest in bacterial therapies in general [89], including the use of genetically modified drug-synthesising bacteria [90], and magnetotactic bacteria [91–93]. Magnetotactic bacteria synthesise multiple aligned nanoscale magnetic particles along their axis in order to align themselves with geomagnetic fields (Fig. 5). This increases their ability to overcome Brownian motion and move in a consistent direction. In environments such as lakes, this is often combined with hypoxia sensing, allowing migration of the bacteria to low-oxygen environments in which they preferentially grow. This hypoxia seeking has been exploited in the development of potential therapies, as it promotes tumour infiltration by the bacteria, which can be detected using MRI [92].
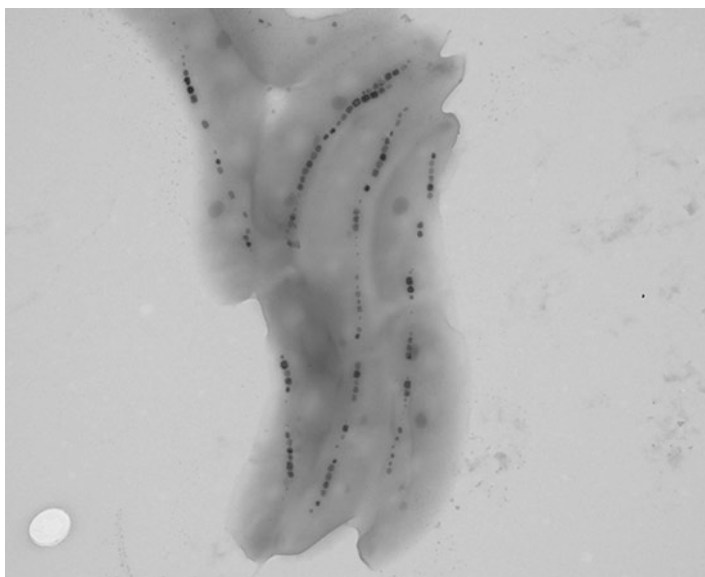

Fig. 5 Transmission electron micrograph showing aligned magnetotactic *Magnetospirillum* sp. bacteria. Individual magnetosomes are made of solid magnetite and appear as dark structures ~40 nm in diameter

Further work has demonstrated that bacteria can be attached to larger molecules such as nanoliposomes or microbeads, which might be useful for tumour drug delivery [94, 95]. One of the advantages of using bacteria to deliver drugs is that a certain amount of self-propulsion can be achieved from the flagellum, which can act together with the directional steering achieved by external magnetic fields. This has been demonstrated using an MRI scanner to steer magnetic bacteria around a maze [8].

Aside from the use of whole magnetotactic bacteria, the magnetic particles (magnetosomes) isolated from these have also been used for a number of applications due to the high quality of their magnetic material. This includes the magnetic targeting of human cells [28], hyperthermia [93], as well as their use as contrast agents for MRI.

6 Imaging Magnetic Particles

A handful of techniques exist for imaging magnetic particles. The most widely available of these is MRI [96], though the more recently developed technique known as magnetic particle imaging (MPI) does offer some advantages such as increased quantification and sensitivity [97], despite the lack of anatomical information that it provides.

6.1 Imaging with MRI

As most commonly used, MRI produces images based on the water proton (^{1}H) signal present in biological tissue. Anatomical detail is provided by differing proton relaxation rates which vary with the composition of different tissues, such as their water, lipid, and solute contents. Further contrast can be produced by the presence of paramagnetic, superparamagnetic, or magnetic particles. MRI has several advantages over other imaging modalities, including the high resolution of the images that can be acquired non-invasively, as well as the structural and functional information that can be obtained. This is illustrated in Fig. 3c–f, which clearly shows the structure of the liver on the left-hand side of the image, along with the tumour, intestines, and abdominal fat. For this reason, both preclinical and clinical magnetic targeting studies have used MRI, demonstrating its utility in the confirmation of particle or cell delivery to the target site [3, 8, 42, 61, 73]. For a more detailed introduction to MRI, see Gadian [96].

Though numerous methods of producing contrast can be achieved with MRI, it is the T_2 and T_2* relaxation mechanisms that are typically most relevant for imaging magnetic particles. T_2 relaxation, also known as transverse relaxation, or spin-spin relaxation, is a measure of the rate at which the net magnetisation in the xy-plane is lost following an RF pulse that flips the net magnetisation into the xy-plane from the z-axis. Specifically, it is the time taken for the signal to decay to 37 % of its initial value following the RF pulse.

Transverse relaxation is influenced by several factors which can be separated out into T_2 and T_2^* effects. Transverse relaxation (T_2) is shorter in environments with high macromolecular content (which appear darker), and longer in tissues with higher water content (which appear brighter), though other factors also affect T_2 relaxation. Magnetic particles appear as hypo-intense (dark) areas on the image, though this results mainly from a T_2^*effect. T_2^* effects, such as magnetic field inhomogeneities, can alter the transverse relaxation rate by increasing the rate at which the de-phasing of spins occurs, and can be separated out from T_2 effects with certain pulse sequences. To reduce the effect of these T_2^* factors, and produce a more T_2-weighted image, a specific type of pulse sequence called a spin echo can be used. To produce a T_2^*-weighted image, which is more sensitive to the detection of super-paramagnetic species such as iron oxides, a gradient-echo sequence can be used in which the de-phasing resulting from T_2 factors is reversed by a magnetic field gradient. These T_2^*-weighted images, however, can be more sensitive to image artefacts caused by non-uniform magnetic fields present in the bore of the magnet.

T_2 contrast agents, such as magnetic particles, shorten the T_2 and T_2^* time of nearby water molecules by de-phasing their spins with the magnetic field inhomogeneities around the particle, thus reducing the amount of signal collected from the surrounding water when the echo is recorded. This results in a hypo-intense or dark area on the image, which indicates the presence of magnetic particles in the tissue (Fig. 3).

The detection of magnetic particles with MRI can be very sensitive, allowing hundreds or fewer to be tracked in optimal conditions [98], and can be further improved by using long imaging times. However, in most settings this is limited by practical considerations such as how long the patient or animal can be kept within the scanner.

The ability to detect magnetic particles can also be complicated and unreliable in certain areas, such as the lungs or haemorrhages, where natural signal voids already occur. Another limitation is the quantification of magnetic particle number, which can also be challenging due to the saturation of contrast produced by focal accumulations of magnetic particles, and reduced detection sensitivity in areas with endogenous signal voids. If quantitative biodistribution data on particle location is required, it is recommended that particles are radiolabelled with isotopes for positron emission tomography (PET), which provides complementary information to MRI in many circumstances. Further information on imaging nanoparticles with other modalities can be found in the relevant chapters in this book.

6.2 Magnetic Particle Imaging

MPI differs from MRI in that the signal is obtained directly from the magnetic particles [97], and not from the effect they have on the spin of nearby water protons. For this reason it has several potential advantages, including the ability to quantify magnetic particle concentration within the host tissue, increased accuracy of identifying regions containing magnetic particles, increased sensitivity, and possibility of performing "multi-color" imaging using magnetic particles. Despite these

factors, however, MPI does not on its own produce anatomical data, and so is best performed alongside CT or MRI imaging, has lower spatial resolution, and is also not yet widely available. A recent review covering the physical principles and nanoparticle tracers for magnetic particle imaging can be found here [99], and also in Chap. 4 of this book by Connolly.

6.3   Multimodality Imaging

Though MRI can enable the non-invasive detection of magnetic particles in the clinic, it does not provide some types of information that would be useful to the development of magnetic targeting techniques, such as whole-body quantitative biodistribution data. Radionuclide imaging (positron emission tomography (PET), and single-photon emission computed tomography (SPECT)) has many of the features also associated with MRI, including their clinical availability and non-invasiveness, and though they provide lower resolution images there are several complementary features. Radionuclide imaging relies on the detection of gamma rays emitted following radioactive decay of isotopes used to label the molecule, particle, or cell of interest. Unlike MRI, these techniques can provide quantitative whole-body detection of labelled molecules, allowing the non-invasive assessment of particle biodistribution to quantify the effects of magnetic targeting procedures. Further information on the design of magnetic particles for radionuclide imaging can be found in Chaps. 10–12. For tracking cells with PET or SPECT, the choice of isotope depends on how long the cells need to be tracked. One option is the use of ^{111}In-oxine (half-life of 2.8 days) and SPECT imaging, which has been used for tracking transplanted cells in the clinic for over 30 years. A recent modification to the technique uses ^{89}Zr-oxine (half-life of 3.3 days) for PET imaging, which could potentially provide better sensitivity and quantification. Both of these techniques can allow cells to be tracked for over a week due to their long half-lives, while the use of other isotopes such as ^{99m}Tc (half-life of 6 h) can be used for cell tracking over shorter periods of time.

7   Conclusions

Despite the numerous challenges involved in implementing magnetic targeting successfully and safely, it remains an exciting and active area of preclinical research due to the wide range of potential clinical applications. In theory, these potentially cover the majority of drug- and cell-based therapies, but in practice this scope will be limited by several physical and biological considerations that have yet to be determined and will be specific to each case. Magnetically targeted delivery offers the ability to simultaneously increase local concentrations of the active agent while reducing systemic dosing and off-target side effects. The inability to balance these so that the

dose in the target organ is sufficient to act therapeutically, while the systemic dose is low enough not to cause unwanted side effects, is the reason why many potential drug candidates fail, and why many approved drugs are limited in their efficacy. For cell therapies, the field is yet to become well established, but the improved treatment response achieved in several preclinical studies from using magnetic targeting demonstrates the potential for its clinical use in the future [2].

References

1. Pankhurst QA, Connolly J, Jones SK, Dobson J. Applications of magnetic nanoparticles in biomedicine. J Phys D Appl Phys. 2003;36(13):R167–81.
2. Connell JJ, Patrick PS, Yu Y, Lythgoe MF, Kalber TL. Advanced cell therapies: targeting, tracking and actuation of cells with magnetic particles. Regen Med. 2015;10(6):757–72.
3. Wilson MW, Kerlan Jr RK, Fidelman NA, Venook AP, LaBerge JM, Koda J, et al. Hepatocellular carcinoma: regional therapy with a magnetic targeted carrier bound to doxorubicin in a dual MR imaging/conventional angiography suite—initial experience with four patients. Radiology. 2004;230(1):287–93.
4. Lubbe AS, Bergemann C, Riess H, Schriever F, Reichardt P, Possinger K, et al. Clinical experiences with magnetic drug targeting: a phase I study with 4′-epidoxorubicin in 14 patients with advanced solid tumors. Cancer Res. 1996;56(20):4686–93.
5. Thomas CR, Ferris DP, Lee JH, Choi E, Cho MH, Kim ES, et al. Noninvasive remote-controlled release of drug molecules in vitro using magnetic actuation of mechanized nanoparticles. J Am Chem Soc. 2010;132(31):10623–5.
6. Cheng K, Shen D, Hensley MT, Middleton R, Sun B, Liu W, et al. Magnetic antibody-linked nanomatchmakers for therapeutic cell targeting. Nat Commun. 2014;5:4880.
7. Grady MS, Howard 3rd MA, Broaddus WC, Molloy JA, Ritter RC, Quate EG, et al. Magnetic stereotaxis: a technique to deliver stereotactic hyperthermia. Neurosurgery. 1990;27(6):1010–5. discussion 5-6.
8. Martel S, Mohammadi M, Felfoul O, Lu Z, Pouponneau P. Flagellated magnetotactic bacteria as controlled MRI-trackable propulsion and steering systems for medical nanorobots operating in the human microvasculature. Int J Robotics Res. 2009;28(4):571–82.
9. Kummer MP, Abbott JJ, Kratochvil BE, Borer R, Sengul A, Nelson BJ. OctoMag: an electromagnetic system for 5-DOF wireless micromanipulation. IEEE Trans Robot. 2010;26(6):1006–17.
10. Pouponneau P, Soulez G, Beaudoin G, Leroux JC, Martel S. MR imaging of therapeutic magnetic microcarriers guided by magnetic resonance navigation for targeted liver chemoembolization. Cardiovasc Intervent Radiol. 2014;37(3):784–90.
11. Riegler J, Lau KD, Garcia-Prieto A, Price AN, Richards T, Pankhurst QA, et al. Magnetic cell delivery for peripheral arterial disease: a theoretical framework. Med Phys. 2011;38(7):3932–43.
12. Nacev A, Beni C, Bruno O, Shapiro B. The behaviors of ferromagnetic nano-particles in and around blood vessels under applied magnetic fields. J Magn Magn Mater. 2011;323(6):651–68.

13. Krishnan KM. Biomedical nanomagnetics: a spin through possibilities in imaging, diagnostics, and therapy. IEEE Trans Magn. 2010;46(7):2523–58.

14. Faraudo J, Andreu JS, Camacho J. Understanding diluted dispersions of superparamagnetic particles under strong magnetic fields: a review of concepts, theory and simulations. Soft Matter. 2013;9(29):6654–64.

15. Song M, Kim YJ, Kim YH, Roh J, Kim SU, Yoon BW. Using a neodymium magnet to target delivery of ferumoxidelabeled human neural stem cells in a rat model of focal cerebral ischemia. Hum Gene Ther. 2010;21(5):603–10.

16. Kobayashi T, Ochi M, Yanada S, Ishikawa M, Adachi N, Deie M, et al. A novel cell delivery system using magnetically labeled mesenchymal stem cells and an external magnetic device for clinical cartilage repair. Arthroscopy. 2008;24(1):69–76.

17. Arbab AS, Jordan EK, Wilson LB, Yocum GT, Lewis BK, Frank JA. In vivo trafficking and targeted delivery of magnetically labeled stem cells. Hum Gene Ther. 2004;15(4):351–60.

18. Sasaki H, Tanaka N, Nakanishi K, Nishida K, Hamasaki T, Yamada K, et al. Therapeutic effects with magnetic targeting of bone marrow stromal cells in a rat spinal cord injury model. Spine. 2011;36(12):933–8.

19. Kyrtatos PG, Lehtolainen P, Junemann-Ramirez M, Garcia-Prieto A, Price AN, Martin JF, et al. Magnetic tagging increases delivery of circulating progenitors in vascular injury. J Am Coll Cardiol Intv. 2009;2(8):794–802.

20. Riegler J, Wells JA, Kyrtatos PG, Price AN, Pankhurst QA, Lythgoe MF. Targeted magnetic delivery and tracking of cells using a magnetic resonance imaging system. Biomaterials. 2010;31(20):5366–71.

21. Kodama A, Kamei N, Kamei G, Kongcharoensombat W, Ohkawa S, Nakabayashi A, et al. In vivo bioluminescence imaging of transplanted bone marrow mesenchymal stromal cells using a magnetic delivery system in a rat fracture model. J Bone Joint Surg Br Vol. 2012;94(7):998–1006.

22. Shen Y, Liu X, Huang Z, Pei N, Xu J, Li Z, et al. Comparison of magnetic intensities for mesenchymal stem cell targeting therapy on ischemic myocardial repair: high magnetic intensity improves cell retention but has no additional functional benefit. Cell Transplant. 2014;24(10):1981–97.

23. Oshima S, Kamei N, Nakasa T, Yasunaga Y, Ochi M. Enhancement of muscle repair using human mesenchymal stem cells with a magnetic targeting system in a subchronic muscle injury model. J Orthop Sci. 2014;19(3):478–88.

24. Vandergriff AC, Hensley TM, Henry ET, Shen D, Anthony S, Zhang J, et al. Magnetic targeting of cardiosphere-derived stem cells with ferumoxytol nanoparticles for treating rats with myocardial infarction. Biomaterials. 2014;35(30):8528–39.

25. Yanai A, Hafeli UO, Metcalfe AL, Soema P, Addo L, Gregory-Evans CY, et al. Focused magnetic stem cell targeting to the retina using superparamagnetic iron oxide nanoparticles. Cell Transplant. 2012;21(6):1137–48.

26. Riegler J, Liew A, Hynes SO, Ortega D, O'Brien T, Day RM, et al. Superparamagnetic iron oxide nanoparticle targeting of MSCs in vascular injury. Biomaterials. 2013;34(8):1987–94.

27. Pislaru SV, Harbuzariu A, Gulati R, Witt T, Sandhu NP, Simari RD, et al. Magnetically targeted endothelial cell localization in stented vessels. J Am Coll Cardiol. 2006;48(9):1839–45.

28. Kang HJ, Kim JY, Lee HJ, Kim KH, Kim TY, Lee CS, et al. Magnetic bionanoparticle enhances homing of endothelial progenitor cells in mouse hindlimb ischemia. Korean Circ J. 2012;42(6):390–6.

29. Cheng L, Wang C, Ma X, Wang Q, Cheng Y, Wang H, et al. Multifunctional upconversion nanoparticles for dual-modal imaging-guided stem cell therapy under remote magnetic control. Adv Funct Mater. 2013;23(3):272–80.

30. Riegler J, Allain B, Cook RJ, Lythgoe MF, Pankhurst QA. Magnetically assisted delivery of cells using a magnetic resonance imaging system. J Phys D: Appl Phys. 2011;44(5).

31. Mathieu JB, Martel S. Aggregation of magnetic microparticles in the context of targeted therapies actuated by a magnetic resonance imaging system. J Appl Phys. 2009;106(4):44904.

32. Alksne JF. Stereotactic thrombosis of intracranial aneurysms. N Engl J Med. 1971;284(4): 171–4.

33. Alksne JF, Fingerhut AG, Rand RW. Magnetic probe for the stereotactic thrombosis of intra-cranial aneurysms. J Neurol Neurosurg Psychiatry. 1967;30(2):159–62.

34. Nacev A, Kim SH, Rodriguez-Canales J, Tangrea MA, Shapiro B, Emmert-Buck MR. A dynamic magnetic shift method to increase nanoparticle concentration in cancer metastases: a feasibility study using simulations on autopsy specimens. Int J Nanomedicine. 2011;6: 2907–23.

35. Vemulkar T, Mansell R, Petit D, Cowburn RP, Lesniak MS. Highly tunable perpendicularly magnetized synthetic antiferromagnets for biotechnology applications. Appl Phys Lett. 2015;107(1):12403.

36. Park JH, von Maltzahn G, Zhang LL, Schwartz MP, Ruoslahti E, Bhatia SN, et al. Magnetic iron oxide nanoworms for tumor targeting and imaging. Adv Mater. 2008;20(9):1630.

37. Wang GK, Inturi S, Serkova NJ, Merkulov S, McCrae K, Russek SE, et al. High-relaxivity superparamagnetic iron oxide nanoworms with decreased immune recognition and long-cir-culating properties. ACS Nano. 2014;8(12):12437–49.

38. Yu F, Zhang L, Huang Y, Sun K, David AE, Yang VC. The magnetophoretic mobility and superparamagnetism of core-shell iron oxide nanoparticles with dual targeting and imaging functionality. Biomaterials. 2010;31(22):5842–8.

39. Yoon TJ, Lee H, Shao HL, Hilderbrand SA, Weissleder R. Multicore assemblies potentiate magnetic properties of biomagnetic nanoparticles. Adv Mater. 2011;23(41):4793.

40. Paquet C, de Haan HW, Leek DM, Lin HY, Xiang B, Tian GH, et al. Clusters of superpara-magnetic iron oxide nanoparticles encapsulated in a hydrogel: a particle architecture generat-ing a synergistic enhancement of the T(2) relaxation. ACS Nano. 2011;5(4):3104–12.

41. Sanson C, Diou O, Thevenot J, Ibarboure E, Soum A, Brulet A, et al. Doxorubicin loaded magnetic polymersomes: theranostic nanocarriers for mr imaging and magneto-chemother-apy. ACS Nano. 2011;5(2):1122–40.

42. Fortin-Ripoche JP, Martina MS, Gazeau F, Menager C, Wilhelm C, Bacri JC, et al. Magnetic targeting of magnetoliposomes to solid tumors with MR imaging monitoring in mice: feasi-bility. Radiology. 2006;239(2):415–24.

43. Doherty GJ, McMahon HT. Mechanisms of endocytosis. Annu Rev Biochem. 2009;78: 857–902.

44. Zhang S, Gao H, Bao G. Physical principles of nanoparticle cellular endocytosis. ACS Nano. 2015;9:8655–71.

45. Petros RA, DeSimone JM. Strategies in the design of nanoparticles for therapeutic applica-tions. Nat Rev Drug Discov. 2010;9(8):615–27.

46. Gratton SEA, Ropp PA, Pohlhaus PD, Luft JC, Madden VJ, Napier ME, et al. The effect of particle design on cellular internalization pathways. Proc Natl Acad Sci U S A. 2008;105(33):11613–8.

47. Thorek DLJ, Tsourkas A. Size, charge and concentration dependent uptake of iron oxide particles by non-phagocytic cells. Biomaterials. 2008;29(26):3583–90.

48. Foged C, Brodin B, Frokjaer S, Sundblad A. Particle size and surface charge affect particle uptake by human dendritic cells in an in vitro model. Int J Pharm. 2005;298(2):315–22.

49. Liu Q, Zhang J, Xia W, Gu H. Magnetic field enhanced cell uptake efficiency of magnetic silica mesoporous nanoparticles. Nanoscale. 2012;4(11):3415–21.

50. Child HW, Del Pino PA, De La Fuente JM, Hursthouse AS, Stirling D, Mullen M, et al. Working together: the combined application of a magnetic field and penetratin for the deliv-ery of magnetic nanoparticles to cells in 3D. ACS Nano. 2011;5(10):7910–9.

51. Dobson J. Gene therapy progress and prospects: magnetic nanoparticle-based gene delivery. Gene Ther. 2006;13(4):283–7.

52. Longmire M, Choyke PL, Kobayashi H. Clearance properties of nano-sized particles and molecules as imaging agents: considerations and caveats. Nanomedicine. 2008;3(5): 703–17.

53. Cole AJ, David AE, Wang JX, Galban CJ, Hill HL, Yang VC. Polyethylene glycol modified, cross-linked starchcoated iron oxide nanoparticles for enhanced magnetic tumor targeting. Biomaterials. 2011;32(8):2183–93.

54. Barenholz Y. Doxil(R)-the first FDA-approved nano-drug: lessons learned. J Contr Release. 2012;160(2):117–34.

55. Zimmermann U, Pilwat G. Organ specific application of drugs by means of cellular capsule systems (author's transl). Z Naturforsch C. 1976;31(11–12):732–6.

56. Wang C, Sun XQ, Cheng L, Yin SN, Yang GB, Li YG, et al. Multifunctional theranostic red blood cells for magnetic-field-enhanced in vivo combination therapy of cancer. Adv Mater. 2014;26(28):4794.

57. Hu CJ, Fang RH, Wang KC, Luk BT, Thamphiwatana S, Dehaini D, et al. Nanoparticle bio-interfacing by platelet membrane cloaking. Nature. 2015.

58. Pouponneau P, Bringout G, Martel S. Therapeutic magnetic microcarriers guided by magnetic resonance navigation for enhanced liver chemoembilization: a design review. Ann Biomed Eng. 2014;42(5):929–39.

59. Fang J, Nakamura H, Maeda H. The EPR effect: Unique features of tumor blood vessels for drug delivery, factors involved, and limitations and augmentation of the effect. Adv Drug Deliv Rev. 2011;63(3):136–51.

60. Cabral H, Matsumoto Y, Mizuno K, Chen Q, Murakami M, Kimura M, et al. Accumulation of sub-100 nm polymeric micelles in poorly permeable tumours depends on size. Nat Nanotechnol. 2011;6(12):815–23.

61. Chertok B, Moffat BA, David AE, Yu FQ, Bergemann C, Ross BD, et al. Iron oxide nanoparticles as a drug delivery vehicle for MRI monitored magnetic targeting of brain tumors. Biomaterials. 2008;29(4):487–96.

62. Podaru G, Ogden S, Baxter A, Shrestha T, Ren S, Thapa P, et al. Pulsed magnetic field induced fast drug release from magneto liposomes via ultrasound generation. J Phys Chem B. 2014;118(40):11715–22.

63. Polyak B, Fishbein I, Chorny M, Alferiev I, Williams D, Yellen B, et al. High field gradient targeting of magnetic nanoparticle-loaded endothelial cells to the surfaces of steel stents. Proc Natl Acad Sci U S A. 2008;105(2):698–703.

64. Shapiro B, Dormer K, Rutel IB. A two-magnet system to push therapeutic nanoparticles. AIP Conf Proc. 2010;1311(1):77–88.

65. Sarwar A, Lee R, Depireux DA, Shapiro B. Magnetic injection of nanoparticles into rat inner ears at a human head working distance. Ieee T Magn. 2013;49(1):440–52.

66. Sarwar A, Nemirovski A, Shapiro B. Optimal Halbach permanent magnet designs for maximally pulling and pushing nanoparticles. J Magn Magn Mater. 2012;324(5):742–54.

67. McNeil RG, Ritter RC, Wang B, Lawson MA, Gillies GT, Wika KG, et al. Functional design features and initial performance characteristics of a magnetic-implant guidance system for stereotactic neurosurgery. IEEE Trans Biomed Eng. 1995;42(8):793–801.

68. Nacev A, Weinberg IN, Stepanov PY, Kupfer S, Mair LO, Urdaneta MG, et al. Dynamic inversion enables external magnets to concentrate ferromagnetic rods to a central target. Nano Lett. 2015;15(1):359–64.

69. Muthana M, Kennerley AJ, Hughes R, Fagnano E, Richardson J, Paul M, et al. Directing cell therapy to anatomic target sites in vivo with magnetic resonance targeting. Nat Commun. 2015;6:8009.

70. Martel S, Mathieu JB, Felfoul O, Chanu A, Aboussouan E, Tamaz S, et al. Automatic navigation of an untethered device in the artery of a living animal using a conventional clinical magnetic resonance imaging system. Appl Phys Lett. 2007;90(11):14105.

71. Alksne JF, Smith RW. Iron-acrylic compound for steriotaxic aneurysm thrombosis. J Neurosurg. 1977;47(2):137–41.

72. Turner RD, Rand RW, Bentson JR, Mosso JA. Ferromagnetic silicone necrosis of hypernephromas by selective vascular occlusion to the tumor: a new technique. J Urol. 1975;113(4):455–9.

73. Kobeiter H, Georgiades CS, Leakakos T, Torbenson M, Hong K, Geschwind JF. Targeted transarterial therapy of Vx-2 rabbit liver tumor with Yttrium-90 labeled ferromagnetic particles using an external magnetic field. Anticancer Res. 2007;27(2):755–60.

74. Chu KF, Dupuy DE. Thermal ablation of tumours: biological mechanisms and advances in therapy. Nat Rev Cancer. 2014;14(3):199–208.

75. Gilchrist RK, Medal R, Shorey WD, Hanselman RC, Parrott JC, Taylor CB. Selective inductive heating of lymph nodes. Ann Surg. 1957;146(4):596–606.

76. Johannsen M, Thiesen B, Wust P, Jordan A. Magnetic nanoparticle hyperthermia for prostate cancer. Int J hyperther. 2010;26(8):790–5.

77. Maier-Hauff K, Ulrich F, Nestler D, Niehoff H, Wust P, Thiesen B, et al. Efficacy and safety of intratumoral thermotherapy using magnetic iron-oxide nanoparticles combined with external beam radiotherapy on patients with recurrent glioblastoma multiforme. J Neuro-Oncol. 2011;103(2):317–24.

78. Bealle G, Di Corato R, Kolosnjaj-Tabi J, Dupuis V, Clement O, Gazeau F, et al. Ultra magnetic liposomes for MR imaging, targeting, and hyperthermia. Langmuir. 2012;28(32): 11834–42.

79. Jordan A, Wust P, Fahling H, John W, Hinz A, Felix R. Inductive heating of ferrimagnetic particles and magnetic fluids: physical evaluation of their potential for hyperthermia. 1993. Int J Hyperther. 2009;25(7):499–511.

80. Heathman TR, Nienow AW, McCall MJ, Coopman K, Kara B, Hewitt CJ. The translation of cell-based therapies: clinical landscape and manufacturing challenges. Regen Med. 2015;10(1):49–64.

81. Fischbach MA, Bluestone JA, Lim WA. Cell-based therapeutics: the next pillar of medicine. Science translational medicine. 2013;5(179):179ps7.

82. Estelrich J, Escribano E, Queralt J, Busquets MA. Iron oxide nanoparticles for magnetically-guided and magnetically-responsive drug delivery. Int J Mol Sci. 2015;16(4):8070–101.

83. Senyei AE, Reich SD, Gonczy C, Widder KJ. In vivo kinetics of magnetically targeted low-dose doxorubicin. J Pharm Sci. 1981;70(4):389–91.

84. Widder KJ, Morris RM, Poore GA, Howard DP, Senyei AE. Selective targeting of magnetic albumin microspheres containing low-dose doxorubicin: total remission in Yoshida sarcoma-bearing rats. Eur J Canc Clin Oncol. 1983;19(1):135–9.

85. Thiele RH, Colquhoun DA, Gillies GT, Tiouririne M. Manipulation of hyperbaric lidocaine using a weak magnetic field: a pilot study. Anesth Analg. 2012;114(6):1365–7.

86. Dames P, Gleich B, Flemmer A, Hajek K, Seidl N, Wiekhorst F, et al. Targeted delivery of magnetic aerosol droplets to the lung. Nat Nanotechnol. 2007;2(8):495–9.

87. Heppner F, Mose JR. The liquefaction (oncolysis) of malignant gliomas by a non pathogenic Clostridium. Acta Neurochir. 1978;42(1–2):123–5.

88. Schmidt W, Fabricius EM, Schneeweiss U. The tumour-Clostridium phenomenon: 50 years of developmental research (Review). Int J Oncol. 2006;29(6):1479–92.

89. Forbes NS. Engineering the perfect (bacterial) cancer therapy. Nat Rev Cancer. 2010;10(11): 784–93.

90. Jiang Y, Sigmund F, Reber J, Dean-Ben XL, Glasl S, Kneipp M, et al. Violacein as a genetically-controlled, enzymatically amplified and photobleaching-resistant chromophore for optoacoustic bacterial imaging. Sci Rep. 2015;5:11048.

91. Martel S, Felfoul O, Mohammadi M, Mathieu JB. Interventional procedure based on nanorobots propelled and steered by flagellated magnetotactic bacteria for direct targeting of tumors in the human body. Conf Proc IEEE Eng Med Biol Soc. 2008;2008:2497–500.

92. Benoit MR, Mayer D, Barak Y, Chen IY, Hu W, Cheng Z, et al. Visualizing implanted tumors in mice with magnetic resonance imaging using magnetotactic bacteria. Clin Canc Res. 2009;15(16):5170–7.

93. Alphandery E, Faure S, Seksek O, Guyot F, Chebbi I. Chains of magnetosomes extracted from AMB-1 magnetotactic bacteria for application in alternative magnetic field cancer therapy. ACS Nano. 2011;5(8):6279–96.

94. Taherkhani S, Mohammadi M, Daoud J, Martel S, Tabrizian M. Covalent binding of nanoli-posomes to the surface of magnetotactic bacteria for the synthesis of self-propelled therapeutic agents. ACS Nano. 2014;8(5):5049–60.
95. Park SJ, Park SH, Cho S, Kim DM, Lee Y, Ko SY, et al. New paradigm for tumor theranostic methodology using bacteria-based microrobot. Sci Rep. 2013;3:3394.
96. Gadian DG. NMR and its applications to living systems, 2nd Edition. Oxford Science Publications. 1996.
97. Gleich B, Weizenecker R. Tomographic imaging using the nonlinear response of magnetic particles. Nature. 2005;435(7046):1214–7.
98. Heyn C, Ronald JA, Ramadan SS, Snir JA, Barry AM, MacKenzie LT, et al. In vivo MRI of cancer cell fate at the single-cell level in a mouse model of breast cancer metastasis to the brain. Magn Reson Med. 2006;56(5):1001–10.
99. Bauer LM, Situ SF, Griswold MA, Samia AC. Magnetic particle imaging tracers: state-of-the-art and future directions. J Phys Chem Lett. 2015;6(13):2509–17.